



Global-scale modeling of glacier mass balances for water resources assessments: Glacier mass changes between 1948 and 2006

Yukiko Hirabayashi ^{a,*}, Petra Döll ^b, Shinjiro Kanae ^c

^a Institute of Engineering Innovation, The University of Tokyo, 2-11-16 Yayoi, Bunkyo-ku, Tokyo 113-0032, Japan

^b Institute of Physical Geography, Frankfurt University, P.O. Box 111932, 60054 Frankfurt am Main, Germany

^c Department of Mechanical and Environmental Informatics, Tokyo Institute of Technology, 2-12-1 O-okayama, Meguro-ku, Tokyo 152-8552, Japan

ARTICLE INFO

Article history:

Received 4 March 2010

Received in revised form 10 June 2010

Accepted 4 July 2010

This manuscript was handled by
Konstantine P. Georgakakos, Editor-in-Chief,
with the assistance of Aiguo Dai

Keywords:

Glacier
Mass balance
Ice volume
Global model

ABSTRACT

Glaciers play an important role for freshwater resources, but in global-scale freshwater assessments, their impact on river flows has not yet been taken into account. As a first step, we developed a global glacier model that can be coupled to global land surface and hydrological models. With a spatial resolution of 0.5° by 0.5° , the glacier model HYOGA computes glacier mass balance by a simple degree-day approach for 50 m sub-grid elevation bands, modeling all glaciers within a grid cell as one glacier. The model is tuned individually for each grid cell against observed glacier mass balance data. HYOGA is able to compute glacier mass balances reasonably well, even those of summer accumulation type glaciers. Still, model uncertainty is high, which is, among other reasons, due to the uncertainty of global data sets of temperature and precipitation which do not represent well the climatic situation at glacier sites. We developed a 59-yr (1948–2006) time series of global glacier mass balance and glacier area by driving HYOGA with daily near-surface atmospheric data. According to our computations, most glaciers have lost mass during the study period. Compared to estimates derived from a rather small number of observed glacier mass balances, HYOGA computes larger glacier mass losses in Asia, Europe, Canadian Arctic islands and Svalbard. In accordance with the estimates, average annual mass losses have increased strongly after 1990 as compared to the 30 yrs before. The sea level equivalent of the melt water from glaciers is 0.76 mm/yr water equivalent after 1990 as compared to only 0.34 mm/yr water equivalent before. We computed an acceleration of glacier mass losses after 1990 for all world regions except South America, where the number of gauge observations of precipitation is very small after 1980.

© 2010 Elsevier B.V. All rights reserved.

1. Introduction

According to the most recent estimate of [Dyurgerov and Meier \(2005\)](#), glaciers and ice caps cover $540,000 \pm 30,000 \text{ km}^2$ outside of Antarctica and Greenland, less than 0.4% of the global land area. Nevertheless, they play an important role in water availability in many river basins. Seasonal water storage in glaciers and ice caps is beneficial for downstream aquatic ecosystems and human water users, as melted ice augments low flows during the warm and dry season. Hereafter, we use the term glaciers to refer to mountain glaciers and ice caps outside of Antarctica and Greenland.

According to [Lemke et al. \(2007\)](#), most glaciers have been shrinking mainly due to air temperature increases, many of them already since 1850. Exceptions are the glaciers in Norway and New Zealand, where glacier mass increased in the 1990s due to increased precipitation, but since the year 2000, glaciers have been shrinking there also. Glacier mass development is driven by the

surface mass balance (the gain or loss of snow, firn and ice over a certain time period) or ice calving, while the mass balance at the glacier bed (loss due to basal melting) is negligible at global or regional scales ([Lemke et al., 2007](#)). At a rate of $0.63 \pm 0.18 \text{ mm/yr}$ water equivalent during 1991–2004, glacier mass loss is estimated to have contributed approximately twice as much to global sea level rise than the melting of the much larger Antarctic and Greenland ice sheets ([Lemke et al., 2007](#)). Future climate change is expected to accelerate glacier shrinkage for most glaciers as precipitation increases cannot balance increased melting due to higher temperatures ([Meehl et al., 2007](#)).

Most global-scale mass balance estimates for glaciers have been based on direct mass balance observations at about 300 glaciers that were up-scaled by area-weighted averaging or spatial interpolation ([Lemke et al., 2007](#)) whereas more than 70,000 glacier locations are recorded in the World Glacier Inventory (WGI), which is collected mainly by the World Glacier Monitoring Service (WGMS), Zurich, and more than 130,000 glaciers are inventoried in [Cogley \(2009\)](#). With a total area of $34,000 \text{ km}^2$, these 300 glaciers represent only about 6% of the global glacier area. [Cogley and Adams](#)

* Corresponding author. Tel.: +81 3 5841 0716.

E-mail address: hyukiko@sogo.t.u-tokyo.ac.jp (Y. Hirabayashi).

(1998) indicated that the method of estimating glacier mass balance by interpolating limited mass balance data lead to a bias. This is due to uneven spatial coverage of observations, because measured glaciers are often small and are commonly located at low elevations due to better accessibility as compared to high elevation glaciers. The total global volume of glaciers outside of Antarctica and Greenland is highly uncertain, with estimates ranging from 51,000 to 166,000 km³ (Lemke et al., 2007; Radić and Hock, 2010).

Several previous studies estimated current variations and future development of glacier mass using numerical mass balance models. For example, Radic and Hock (2006) developed a mass balance glacier model of Storglaciären in Sweden and projected future glacier mass development. Verbunt et al. (2003) applied their numerical snow and glacier model to estimate time series of glacier volume in Alpine river basins. Rees and Collins (2006) showed the effect of climate warming on discharge in glacier-fed Himalayan Rivers, using a three-dimensional glacier model coupled with a hydrological model. Huss et al. (2008) developed a distributed mass balance and glacier evolution model and applied the model to assess the impact of climate change on runoff from three highly glacierized catchments in Switzerland. However, these studies treated a limited number of glaciers with mostly well-observed mass balances. In a global-scale study, Raper and Braithwaite (2006) estimated the impact of climate change on glacier mass by first estimating the 1961–1990 average mass balance in 1° grid cells, using modeled glacier mass balances in seven glacier regions with good mass balance observation and a multiple regression of gradients of mass balance versus altitude on global gridded estimates of long-term average precipitation and summer temperature. Then they scaled their computed 1961–1990 global mass balance to match the previous estimate, and projected the future global mass balance using temperature projections from two different climate models. Hock et al. (2009) also used a modeling approach to obtain global and regional scale glacier mass balance estimates for the period 1961–2004, based on modeled mass balance sensitivities to temperature and precipitation changes as well as long-term temperature and precipitation trends obtained from reanalysis.

To estimate the impact of glaciers on river discharge worldwide, it is necessary to determine not only long-term average annual glacier mass balances but daily or monthly time series. Only such time series will make it possible to better estimate the impact of climate change on seasonal low flows and droughts in glacier-fed river basins. In modeling studies that did not take into account glaciers, many glacier-fed river basins were projected to suffer from increases in drought frequency induced by climate change (e.g. Hirabayashi et al., 2008a; Lehner et al., 2006). To the best of our knowledge, no numerical mass balance models have been developed up to now that can provide gridded sub-annual time series of glacier mass changes for the whole globe.

The aim of the study presented here is to develop a global glacier model for estimating daily gridded time series of glacier mass balances, suitable for supporting global water resources assessments. The output of our new global glacier model HYOGA ("glacier" in Japanese) can be used to drive global hydrological or land surface models. This will allow us, for the first time, to assess the impact of glaciers on freshwater resources at the global scale, also under conditions of climate change. Since a high percentage of irrigated areas are located in glacier-fed river basins, HYOGA also has the potential to improve global food security assessments. Besides, model results could also be used for estimating the contribution of glaciers to sea level rise.

In the following section, we first describe the model and its input data, and then show how the model was initialized and calibrated such that the time series of glacier mass balance between 1948 and 2006 could be computed. In Sections 3 and 4, modeled

glacier mass changes are presented, and model uncertainties are discussed. In Section 5, we summarize our work and draw conclusions.

2. Methods

2.1. Model description

The global glacier model HYOGA is driven by time series of daily precipitation and near-surface temperature and computations are performed using daily time steps. The horizontal spatial resolution of HYOGA is 0.5° by 0.5° as most global hydrological models, and many climate data sets, share this resolution. All glaciers within each grid cell are modeled as one equivalent glacier, the area of which is the sum of the areas of all glaciers within the grid cell. Volume-area scaling is used to estimate glacier volume from (observed) glacier area, and to update glacier area after the computation of glacier mass and thus volume changes after each time step.

Mass balances of snowpack and glacier ice are determined in 50 m sub-grid elevation bands, using a simple degree-day approach to compute melting. Within each grid cell, the air temperature is assumed to decrease with increasing altitude, with a constant lapse rate of $-0.65^{\circ}\text{C}/100\text{ m}$. This value was determined by comparing 63 modeled and observed glacier mass balances at different elevation bands (observations provided by WGMS). With this value, which is equal to the value used by Braithwaite and Raper (2007), it was possible to obtain modeled equivalent line altitudes that are similar to observed values. Like temperature, precipitation varies with altitude, but these variations are very site specific, depending, among others, on wind direction and orography. Therefore, it is not possible to use a uniform precipitation lapse rate, and a suitable approach for determining precipitation lapse rates for global-scale studies does not exist yet. Thus, precipitation was assumed to be the same in all elevation bands of a grid cell. Potential orographic effects on precipitation amount are however indirectly adjusted via the calibration process explained in Section 2.3.2.

2.1.1. Mass balances

HYOGA includes two mass balance modules: a snowpack module which simulates the accumulation and melting of snow as well as the transformation of snow into glacier ice, and a glacier module which computes the volume of melted glacier ice using a simple degree-day approach. The mass balance of the snowpack in the i th elevation band (Fig. 1) is computed in terms of equivalent liquid water volume as

$$\begin{aligned} Sn_i(t + \Delta t) &= Sn_i(t) + Snf_i(t) - G_i - M_{si} \\ M_{si} &= (T_i - T_0) \cdot DDF_{snow} \text{ if } T_i > T_0 \\ &\quad 0 \text{ otherwise} \end{aligned} \quad (1)$$

where Sn_i is water equivalent of snowpack, t is time, Δt is 1 day, Snf_i is snowfall, G_i is the volume of water that is transformed from snow into glacier ice, M_{si} is volume of melted snow, T_0 is a critical temperature for snow melting, T_i is surface temperature at the sub-grid elevation band height and DDF_{snow} is the degree-day factor of the snowpack. T_0 was set to 0 °C, while DDF_{snow} was adjusted by calibration (see Section 2.3.2). We assume that only precipitation that falls as snow affects the snowpack balance. If HYOGA is linked to a hydrological model, rainfall on glaciers immediately becomes runoff. Precipitation is assumed to fall as snow if air temperature of the elevation band is less than or equal to 2 °C. This threshold was used because it leads to similar global snowfall amounts as a more sophisticated method that considers humidity (Hirabayashi et al., 2008c). One year after snowfall is incorporated into the snowpack, it is transformed into glacier ice (Fig. 1). Thus, firn is not taken

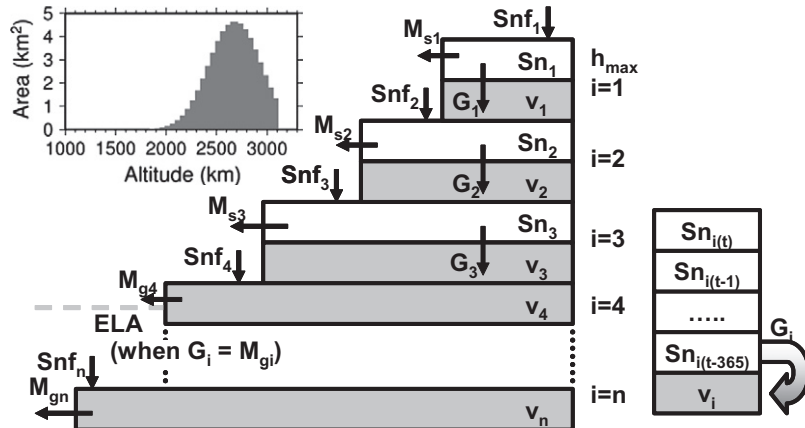


Fig. 1. Schematic of vertical glacier structure and flows assumed in HYOGA. i is number of elevation band, Snf is snowfall, M_s is snow melt, M_g is glacier melt, G is mass of snow transformed to ice, S_n is volume of snowpack and v is volume of ice. In this example, snow layers exist only in the three uppermost 50 m elevation bands. The small diagram on the right represents that snow is assumed to become glacier ice 1 yr after snowfall. The upper left panel shows, as an example, the area-altitude relationship of a glacier grid located in the Alps (10.25E, 46.75 N), as assumed by HYOGA, with maximum and minimum glacier altitude of 3075 m and 1875 m, respectively, and a total area of 55.41 km².

into account in HYOGA. The initial value of Sn_i on January 1st, 1948, was obtained by a spin-up simulation from 1948 to 1990, starting with zero snow volume on January 1st, 1948. Sn_i on December 31st, 1990, as computed by the spin-up simulation, is then used as initial value of Sn_i .

The mass balance of the glacier ice in the i th elevation band is computed as

$$\begin{aligned} v_i(t + \Delta t) &= v_i(t) + G_i - M_{gi} \\ M_{gi} &= (T_i - T_0) DDF_{ice} \quad \text{if } T_i > T_0, \text{ and } S_i(t) = 0 \\ &0 \text{ otherwise} \end{aligned} \quad (2)$$

where v_i is volume of glacier, M_{gi} is the volume of glacier melt, and DDF_{ice} is the degree-day factor of ice melting. As for the snowpack, T_0 is set to 0 °C. Melting of the glacier ice in an elevation band is assumed to occur only if there is no snowpack in this elevation band. The initial value of v_i on January 1st, 1948 was obtained iteratively based on data on glacier areas and a volume-area relation (comp. Section 2.1.2) as described in Section 2.3.1.

By summing the computed glacier mass changes of all the elevation bands, the total glacier volumes in each grid are computed for each day. Volume-area scaling is used to compute the resulting changes in glacier area (comp. Section 2.1.2). The model was calibrated by fitting the modeled glacier mass balance to observed glacier mass balance data.

2.1.2. Vertical glacier structure

All glaciers within a grid cell are simulated as only one glacier that is described by the glacier area (and volume) in each 50 m elevation band (Fig. 1). The glacier area in each elevation band is estimated as follows. The maximum possible glacier area at the i th elevation band $amax_i$, in km², is determined using a normal distribution curve which is shifted by one third of the range of glacier altitudes ($h_{\max} - h_{\min}$) as

$$amax_i = r/\sqrt{2\pi}s \times \exp[-\{h_{\max} - h_i - (h_{\max} - h_{\min}/3)\}^2/2s^2] \quad (3)$$

where r is a coefficient, h_i is the mean altitude of the i th elevation band, in m, h_{\max} and h_{\min} are the maximum and minimum glacier altitude, in m, respectively, and s is a parameter that is set to 2.

Eq. (3) is derived from the vertical glacier area distribution of the Dongkemadi Glacier in Tibet (Fujita et al., 2007) and the glacier model of Rees and Collins (2006) who modeled a hypothetical alpine glacier. We adjusted h_{\max} and h_{\min} by calibration as described in Section 2.3.2. Initial values were taken from WGI where avail-

able; otherwise h_{\max} was set at the maximum cell elevation, while h_{\min} was assumed to be equal to ELA – ($h_{\max} - ELA$).

ELA is the long-term average equilibrium line altitude where glacier accumulation equals ablation (melting), and Braithwaite and Raper (2007) showed that long-term averages of ELAs and median glacier elevations are very similar. Preliminary ELAs were computed by a HYOGA model run from 1948 to 1980, with preliminary values of h_{\max} and h_{\min} , and degree-day factors for snow and ice of 3 and 5 mm/°C/day, respectively. In some grid cells, no ELA could be computed because modeled mass balances of all elevation bands showed the same sign. Then, initial h_{\min} was set equal to the lowest grid elevation. As elevation data, we used the 30 arc sec (approximately 900 m) elevation data of the Shuttle Radar Topography Mission (SRTM30 data). The coefficient r is adjusted such that the initial sum of $amax_i$ is equal to the initial glacier area within the grid cell.

If $amax_i$ is larger than the sub-grid area of the i th elevation band $aband_i$, the difference between $amax_i$ and $aband_i$ is summed to the $amax$ of the next lower elevation band. In order to minimize required disk space and computational cost, $aband_i$ of each elevation band was determined from the cell area with elevations below h_i

$$\sum_{k=1}^i aband_k = A_{cell} \cdot (\log(h_i) - \alpha)/\beta \quad (4)$$

where A_{cell} is total area of the 0.5° grid cell, in km². Parameters α and β were obtained by fitting Eq. (4) to SRTM30 elevation data within each 0.5° grid cell, with the global mean correlation coefficient exceeding 0.98. Glacier area at the i th elevation band ($amax_i$) is then obtained by distributing total glacier area per grid cell (A) starting from the highest elevation band and proceeding downward. The $amax_i$ is fixed except for the lowest glacier elevation band. $amax_i$ is fixed for the whole HYOGA simulation, except for the elevation bands located at and below the lowest band with glacier. $amax_i$ in the lowest glaciated band is calculated as A minus total glacier area located above the lowest glaciated elevation bands. The values of $amax_i$ at the elevation bands below the lowest glaciated band are set to $aband_i$. A is updated after each time step based on the new total glacier volume using the following equation:

$$A = (V/c_a)^{1/\gamma} \quad (5)$$

where V is total glacier volume in each 0.5° grid cell, in km³. $\gamma = 1.375$ from Bahr et al. (1997) and $c_a = 0.2055 \text{ m}^{3-2\gamma}$ from Chen and Ohmura (1990) are used for all glaciers. If A increases, the additional glacier area is allocated to the lowest elevation band up to the

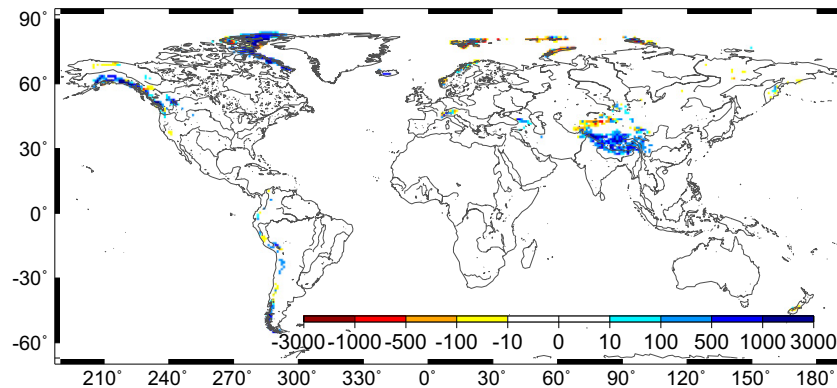


Fig. 2. Difference of glacier areas according to GGHYDRO and WGI: GGHYDRO area minus WGI area in each 0.5° grid cell, in km^2 .

maximum area of the elevation band ($a_{\max i}$). Representative glacier altitude in the lowest elevation band is assumed to be the middle altitude of the elevation band. If A decreases, glacier area is decreased in the lowest elevation band.

With its approach of daily updating of glacier areas per elevation band, HYOGA takes account of the feedback between changes in glacier area, glacier elevation and glacier mass balance. Although the time scale associated with the feedback processes of glacier geometry is much longer than daily, HYOGA updates glacier area in every daily time step. If the ice in a grid cell shrinks, it persists only in the higher elevation bands, and melting per unit glacier area becomes smaller. Since the area and the area-related volume of glacier at each elevation band are updated every day, the model accounts only implicitly for glaciers. The potential positive feedback of a decreasing glacier surface elevation due to glacier thinning is not taken into account.

2.2. Data

Input data for HYOGA are time series of gridded daily near-surface air temperatures and precipitation as well as calculated initial glacier areas. The observed glacier mass balances at specific points in time are used for calibration procedures.

2.2.1. Climate input

A global 0.5° gridded data set of daily precipitation and near-surface temperature for 59 yrs from 1948 to 2006 (Hirabayashi et al., 2005; Hirabayashi et al., 2008b) was used to drive the glacier model. The precipitation data are corrected for gauge errors (based on daily meteorological data and information on gauge types, Hirabayashi et al., 2008c). The temperature data set is based on monthly temperatures of Fan and van den Dool (2008) that are topographically adjusted, and is called H08-FV. An alternative data set of daily surface temperature, called H08-CRU, which is based on monthly temperature values of the Climate Research Unit version TS 2.1 data set (CRU; Mitchell and Jones, 2005), was generated by also using the method of Hirabayashi et al. (2008b). Since temperature data of CRU are available up to 2002 only, monthly temperatures during 2003–2006 in H08-CRU were computed from monthly temperature data of Fan and van den Dool (2008) for this period by scaling with the mean ratio of monthly temperatures of CRU and Fan and van den Dool (2008) from 1986 to 2002. This time period was chosen as both the CRU and Fan and van den Dool data sets are based on a large number of measurement stations during this period.

2.2.2. Glacier areas

A 0.5° gridded global glacier area data set was created by aggregating glacier area data of the World Glacier Inventory (WGI) and the Global Hydrological Data (GGHYDRO, Release 2.3, available on

line from <http://www.trentu.ca/geography/glaciology>; Cogley, 2003). These data sets represent spans of time rather than dates. They are used to estimate initial glacier areas in 1948 (compare Section 2.3).

WGI provides observation data of about 70,000 glaciers, including glacier location, area, elevation and observation dates. GGHDRO provides total area of glacier on a global 1° grid and was generated based on maps, mainly at the 1:1,000,000 scale, that had been published over several decades in the mid-20th century. We assumed that the glacier area of GGHDRO represents glacier area information before 1977. Glacier area of WGI per 0.5° grid cell is mostly smaller than that of GGHDRO, probably because WGI does not cover all glaciers in those cells. Glacier information in WGI is limited to about 30% of global glacier area outside of Greenland and Antarctica. In many grid cells, GGHDRO indicates glaciers while no information is available in WGI (Fig. 2). These grid cells are found in Europe, Central Asia, the Himalaya, Peru, Chile and the southern coastal glaciers of Alaska. In some cells, WGI glacier area is larger than GGHDRO glacier area (e.g. in some parts of Alaska, Peru and Chile, and of the Tibetan Plateau) (Fig. 2). A possible reason for this is that GGHDRO expresses glacier area as integer percentages of total 1° cell area. Thus resolution is 1% of grid cell areas, and glaciers smaller than that (approx. 100 km^2 at the equator) are not included.

We combined these two products by first disaggregating GGHDRO to the 0.5° grid using SRTM30 sub-grid altitude information. The four sets of 3600 SRTM30 sub-grid elevations per 0.5° cell were sorted, and the glacier area in each 1° GGHDRO grid cell was disaggregated to the four 0.5° grid cells by allocating glacier area preferentially to the highest elevations. In the second step, individual glacier area data of WGI were summed for each 0.5° grid and compared to GGHDRO-based 0.5° glacier area. Finally, the greater of the two values for each grid cell was included in our global glacier area data set. Glaciers on small Arctic islands not covered by the climate data sets were not taken into account in the glacier area data set.

Among the approximately 60,000 0.5° land cells, only 2613 contain glaciers. Table 1 compares our 0.5° glacier area data set with other published estimates of glacier areas that exclude glaciers and ice sheets in Antarctica and Greenland. Total glacier area of this study is $534,945 \text{ km}^2$, which is similar to other published data sets. In our data set, glacier areas on North American Arctic Islands and on Sub-Antarctic islands are smaller than in other data sets, because 0.5° grid cells with small islands but without data in the global meteorological data sets we used were excluded from our analysis.

2.2.3. Glacier mass balance observation

A total of 110 observed time series of annual mass balances for individual glaciers, from Dyurgerov and Meier (2005) (referred to as DM05) and, for New Zealand only, from Heydenrych et al.

Table 1
Comparison of different estimates of the global distribution of glacier and ice cap area outside of Greenland and Antarctica, in km², based on Braithwaite and Raper (2002), Dyurgerov and Meier (2005) and Radić and Hock (2009). Alaska in the table includes glaciers in northwestern Canada. The last column indicates the regions distinguished in Fig. 8.

	Meier (1984)	Haebler et al. (1989)	Oerlemans (1993)	Braithwaite and Raper (2002)	Dyurgerov and Meier (1997)	Dyurgerov and Meier (2005)	Radić and Hock (2010) ^b	This study
Arctic Canada	150,600	151,758	149,900	153,184	244,500 ^a	151,800	14,690	139,922 f
Arctic Eurasia	56,100	56,135	55,696	60,723	n.a.	n.a.	56,781	70,656
Europe (Mainland)	6000	6095	5625	6758	18,000 ^a	17,286	6102	9022 e
Iceland	11,300	11,260	10,938	11,160	n.a.	n.a.	10,671	11,005
W. Canada and W. US	125,210	124,342	109,680	101,505	49,000 ^a	129,300	21,480	44,949 b
Alaska	38,800	36,612	36,612	33,685	74,700 ^a	79,260	56,213	36,305 g
Svalbard	n.a.	10	11	n.a.	36,600	36,612	n.a.	11
Africa	111,900	129,076	117,129	121,711	n.a.	n.a.	118,629	128,444 d
Former USSR and Asia	1000	860	1007	433	119,000 ^a	121,575	1156	1158
Australasia	36,260	25,908	36,298	31,521	35,000	25,000	36,700	36,099 c
S. America	5000	7000	5000	2646	5000	5000	3740	1497 h
Sub-Antarctic islands	500,910	516,148	486,598	489,159	576,800	486,598	518,048	534,945 a
Total area excluding Greenland and Antarctica								

n.a.: Not available.

^a Regions for which regional averages of mass balance by Dyurgerov and Meier (1997) were used for calibration.
^b Aggregated from original values of Table 2 by Radić and Hock (2010); sum totals of their original region 2 and 3 (Europe), 4, 5 and 6 (Arctic Eurasia), 7, 8, and 9 (Asia) and 14 and 15 (South America).

(2004), were used for the calibration of HYOGA. Two thirds of the about 300 observed glacier mass balances could not be used for calibration, because there were several glaciers with observations within the same 0.5° grid cell. Data for the glacier with the largest area were selected if there was more than one observed glacier. Mean length of the available mass balance observations was 13 yrs. The 110 grid cells with observed glacier mass balances are mainly in Europe (33), USA and Canada (30) and Asia (22). Only two are located in South America, while the rest are located in Svalbard (9), Canadian Arctic islands (6) and Sub-Antarctic islands (1). Yearly glacier mass balances averaged over large regions of Serreze et al. (2000), which provide an update of Dyurgerov and Meier (1997), were also used for model calibration and validation (referred to as DM97). For validation, summer and winter mass balance observations were available for 21 glaciers (it is not always the same as the 110 glaciers with annual data used for calibration, as it was sometimes not the largest glacier in a grid cell that had summer and winter data available).

The hydrological year starts when glacier melt reaches its minimum. In this study, the hydrological year starts on the 1st of October in the northern hemisphere and on the 1st of April in the Southern Hemisphere.

2.3. Model initialization and calibration for estimating global glacier mass balance from 1948 to 2006

Glacier areas in 1948 were estimated by HYOGA in an iterative manner, based on observed glacier areas for which the observation time varies between grid cells. HYOGA was calibrated against observed glacier mass balances, adjusting four model parameters: the maximum and minimum glacier altitude h_{max} and h_{min} , and the melting factors DDF_{ice} and DDF_{snow} . Computation of initial glacier areas and calibration had to be done jointly, as initial areas depend on the calibration parameters.

2.3.1. Initialization of glacier area

Since the global glacier area data set (see Section 2.2.2) contains observations in different years and months, it was necessary to estimate, as initial condition, the glacier area in each grid cell on the 1st of January 1948, the start of meteorological data. We prepared gridded data sets of the year and month when the glacier area was observed, using the glacier statistics of WGI. WGI provides information of observed year (about 30,000 glaciers) and month (about 26,000), respectively. However, date information of WGI is rather inhomogeneous, providing, e.g. dates of snowline observation, of map publication or of areal photography. If there was more than one glacier with information on observation date within grid cell, data of the largest glacier was used. If observation dates were not available, those of neighboring grids were used. If there is not even information for the neighboring grids, observation date was set to the 1st of January 1975, because about 24,000 WGI stations were observed during the period 1961 and 1980 (compare Fig. 2 of Cogley, 2009). The glacier area on the 1st of January 1948 was then obtained iteratively for each of the 2613 grid cells with glaciers, using different initial glacier areas until the HYOGA glacier mass balance led to a glacier area on the respective observation date that did not differ by more than 5% from the observation. Initial glacier area of each grid cell was updated in each calibration round, using the respective values of the four calibration parameters. The initial glacier areas that were finally adopted were obtained with the calibrated values of the calibration parameters.

2.3.2. Model calibration

HYOGA was calibrated against long-term average annual glacier mass balances observed within the time period 1948–1980, for the

available observation period, because glacier mass before 1980 is more stable than afterwards. The calibration against observed mass balances of individual glacier is problematic as HYOGA does not compute the mass balance of individual glaciers but lumps all glaciers within one grid cell into one equivalent glacier. We thus assume that all glaciers within each grid cell have the same specific mass change (mass change divided by glacier area).

Calibration was done in two steps by first adjusting maximum and minimum glacier altitude h_{max} and h_{min} in Eq. (3) and then, in a second step, the degree-day factors (DDF_{snow} and DDF_{ice}) in Eqs. (1) and (2). In each step, the parameters were adjusted against the cell-specific long-term average of total glacier mass balance observed in 110 grid cells, taking into account all available observation periods before 1981. If there were no mass balance observations within 10 grid cells from the target cell, and the glacier grid cell was located within one of the five regions with available data (see regions with asterisk in Table 1), average regional mass balances for 1961–1993 of DM97 were used for calibration. These regional balances were obtained as the area-weighted means of observed mass balances. A 948 out of the 2613 glacier grid cells were calibrated against these regional estimates of long-term glacier mass balance. For 190 grid cells in South America, Australasia, Africa, Sub-Antarctic islands and small arctic islands, the long-term average mass balance 1948–1980 was assumed to be zero for calibration purposes.

During calibration, variation of h_{max} and h_{min} was constrained only by the maximum and minimum elevation within the grid cell, respectively. The degree-day factor of snow (DDF_{snow}) was allowed to range from 1 to 4 mm/°C/day. This range includes the values that are used in global hydrological models (e.g. Döll et al., 2003) and numerical glacier models (e.g. Rees and Collins, 2006). The degree-day factor of glacier ice (DDF_{ice}) was adjusted between 3 and 20 mm/°C/day, until the long-term average yearly mass balance was as close as possible to the observed mass balance. This range for DDF_{ice} is based on the literature (e.g. Jóhannesson et al., 1995; Singh et al., 2000; Hock, 2003; Zhang et al., 2006).

Fig. 3 compares modeled and observed long-term average specific glacier mass changes, considering the whole observation period and not just the calibration period which ended in 1980. Using H08-CRU temperature data (Fig. 3, left), at least 15 glaciers show far too negative mass balances even after calibration, i.e. the glaciers shrink much too rapidly in the model. These glaciers are located in High Mountain Asia and in mountainous areas in the US, Canada, and Alaska, and often in areas where H08-CRU temperatures are significantly higher than the H08-FV values. This is partic-

ularly the case in arid and semi-arid Asia. The warm bias of CRU temperature in summer caused glaciers in High Mountain Asia to have no snowfall in summer even on the top of mountains. Because many arid and semi-arid glaciers in Asia show both accumulation and melting in the summer monsoon season (Fujita and Ageta, 2000), glaciers in these regions are particularly sensitive to potential temperature biases. We concluded that the H08-FV temperature product of Fan and van den Dool (2008) is preferable for estimation in most regions in Asia. H08-FV, however, also leads to problematic mass balances, outside of Asia (Fig. 3, center). When HYOGA was calibrated using either the H08-FV or the H08-CRU precipitation data set, H08-FV led to better calibration results in half of the grid cells with glaciers, and H08-CRU in the other half. In our further analysis, we selected for each of the 2613 grid cells with glaciers the temperature data set that, after calibration, led to a better fit to the observed mass balances. With this approach, referred to as H08-mix, modeled mass changes are less biased, with an average relative root mean square error of modeled mass change among the 110 observed glaciers of 54% as compared to that of simulations using H08-CRU (230%) and H08-FV (197%) (Fig. 3 right). These large root mean square errors of H08-CRU and H08-FV are due to about 30 of the 110 observations where snowfall is underestimated and glacier melting is overestimated due to high temperature values. About 1300 of the 2613 grid cells show differences of less than 5% for both H08-FV and H08-CRU after the calibration process. In H08-mix, which is used for further computations, 1485 of the computed grid cell balances differ by less than 5% from the glacier balances of neighboring observed glacier or from the regional averages.

For 21 glaciers, relatively long-time series of summer and winter mass balances were obtained from the World Glacier Monitoring Service (WGMS). These data are compared to summer and winter mass balances as computed by HYOGA for the respective grid cells and time periods. We assumed that summer and winter mass changes refer to the periods 1st April–30th September and 1st October–31st March, respectively (except for the one observation located in Southern Hemisphere).

Fig. 4 indicates that HYOGA cannot simulate well the observed seasonality of winter accumulation and summer ablation. It computes smaller summer mass losses than are observed, and barely computes any winter mass gains. A likely reason for the underestimation of winter accumulation is an overestimation of winter temperature or an underestimation of winter precipitation in the global climate data set that we used. In a study of glaciological conditions in seven regions, Braithwaite and Raper (2007) found it

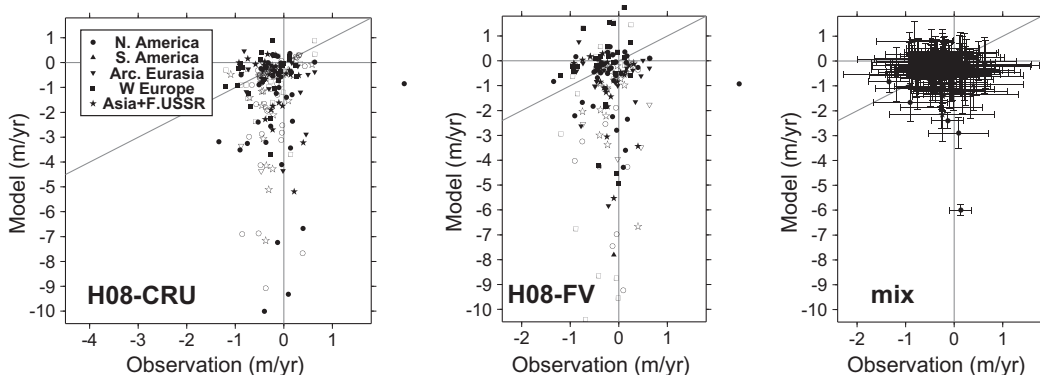


Fig. 3. Comparisons of modeled and observed average annual glacier mass changes during the respective observation periods, using temperature data of H08-CRU (left), of H08-FV (center) or a mix of temperature data of H08-CRU and H08-FV temperature data (right). Each symbol indicates glacier mass changes at one of 110 grid cells with observations by DM05. Observed values relate to the largest glacier within the grid cell, modeled values to the total glacier mass within the grid cell. Open symbols: before the calibration, filled symbols: after calibration. The error bars represent the standard deviation of annual mass balance values during the observation periods. Diagonal grey lines indicate where model and observation are equal.

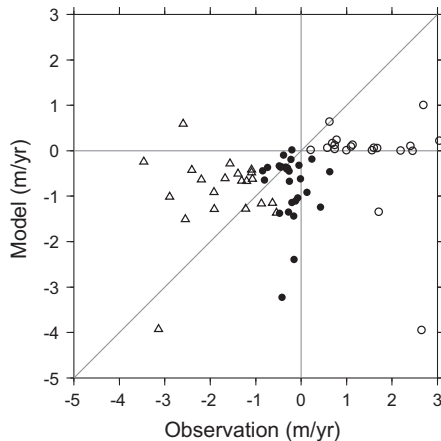


Fig. 4. Comparison of modeled and observed average annual, summer and winter glacier mass (snowpack and ice) changes for 21 grid cells during the respective observation periods. Observed values relate to either the largest glacier within the grid cell or, if no data were available, to another glacier within the grid cell, modeled values to the total glacier mass within the grid cell. Filled circles: annual mass balance, open triangle: summer mass balance, open circle: winter mass balance.

necessary to decrease temperature data of a global data set empirically using observed temperature at the respective glacier sites.

For three example glaciers/grid cells, Fig. 5 shows time series of observed and computed annual mass balances. Modeled mass balances show less interannual variability than of the observed balances, even though average annual mass balances are similar due to the calibration process. Discrepancies between modeled and observed mass balances are, on the one hand, caused by the fact the observed mass balances are values for single glaciers, while modeled values represent the average over all glaciers located within the grid cell. Thus, even if the model represented glacier mass changes at the scale of grid cells perfectly, model results would only fit to the selected observations if all glaciers in the grid cell had the same specific mass balances. On the other hand, inadequate climate data and the modeling of glacier distribution within grid cells are also major causes for the discrepancies.

3. Results

Fig. 6 (top) presents a global map of 0.5° gridded estimates of glacier area on the 1st of January 1948 as derived by an iterative spin-up simulation with HYOGA. Glacier area per grid cell is large in high latitudes (e.g. Canadian and European arctic islands) and in the Himalayas. Globally, 76% of the 2613 0.5° glacierized cells show glacier areas below 300 km² (about one tenth of the cell area) in 1948, while 33% of the glacierized grid cells have a glacier area of

less than 50 km². Global glacier area was estimated as 534,893 km² in 1948, compared to the value of 534,945 km² in the basic data compiled for this study which mixes glacier areas from different points in time (comp. Section 2.2.3; values shown in Table 1). Global glacier area was simulated to have decreased by 0.8% between 1948 and 2006. This corresponds to an average annual value of areal shrinkage of 0.014%/yr, which is only about a fifth of the rate derived by extrapolation of repeated measurements of glacier areas (Cogley, 2008).

Fig. 6 (bottom) shows a global map of the average annual specific mass change from 1948 to 2006, while Fig. 7 provides enlarged views of selected regions. Here, the mass change is derived as mass change of glacier (expressed as volume of liquid water) divided by the glacier surface area of the particular year, in mm/yr. It is obvious that most glaciers suffered from mass losses (retreat of glacier) in the last decades, but there is a high spatial variability, even with glacierized grid cells with mass gains located next to grid cells with high mass losses (e.g. in Norway and South America). In Norway, for example, such a high spatial variability of mass loss is reasonable, because there is a steep gradient between western maritime (gaining) to eastern continental (loosing) glaciers. The amount of decrease of total glacier volume (not shown) is particularly large in High Mountain Asia, the coastal zone of Alaska and the European Arctic islands. Fig. 8 shows time series of annual glacier mass changes as global average and for seven large regions (comp. Table 1) for the time period 1948–2006, comparing modeled values to independent estimates of mass balances from DM05 and DM97. DM05 obtained their regional and global estimates of by area-weighted averaging time series of observed mass balances of a total of about 300 glaciers, while DM97 only used about 250 glaciers. All regions except South America show significant mass losses for both model estimation and observation. The differences of the ranges of mass balance variation among different regions as estimated by DM05 and DM97 are fairly well replicated by HYOGA.

Regionally averaged mass losses in South America (Fig. 8) are relatively small, because there are some grid cells with large glaciers in the southern part of South America, which show a glacier mass increase. However, our model results for South America suffer from a strong decrease in precipitation observations after 1980 (see Section 4), which may partly explain discrepancies to DM05 but also satellite-based studies of Rignot et al. (2003) and Chen et al. (2007).

Table 2 compares the modeled global total specific mass balance and its equivalent sea level rise in mm/yr with values of observation-based estimates that are the arithmetic means of estimates by DM05 and two other data sets which together take into account 221–470 mass balance measurements within each 5-yr time period analyzed (Lemke et al., 2007, their Table 4.4 and their Fig. 4.14). Global glacier mass loss values as computed by HYOGA

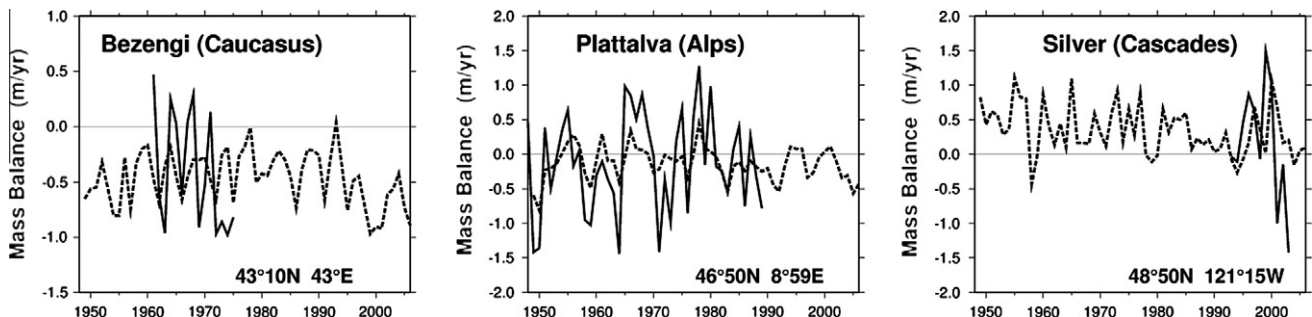


Fig. 5. Examples of annual specific mass balances of three selected glaciers: Bezenji glacier in the Caucasus (left), Plattalva glacier in the Alps (middle) and Silver glacier in the Cascades, USA (right). Solid lines indicate observations, and dotted lines indicate HYOGA model results for the grid cells in which the observed glaciers are located.

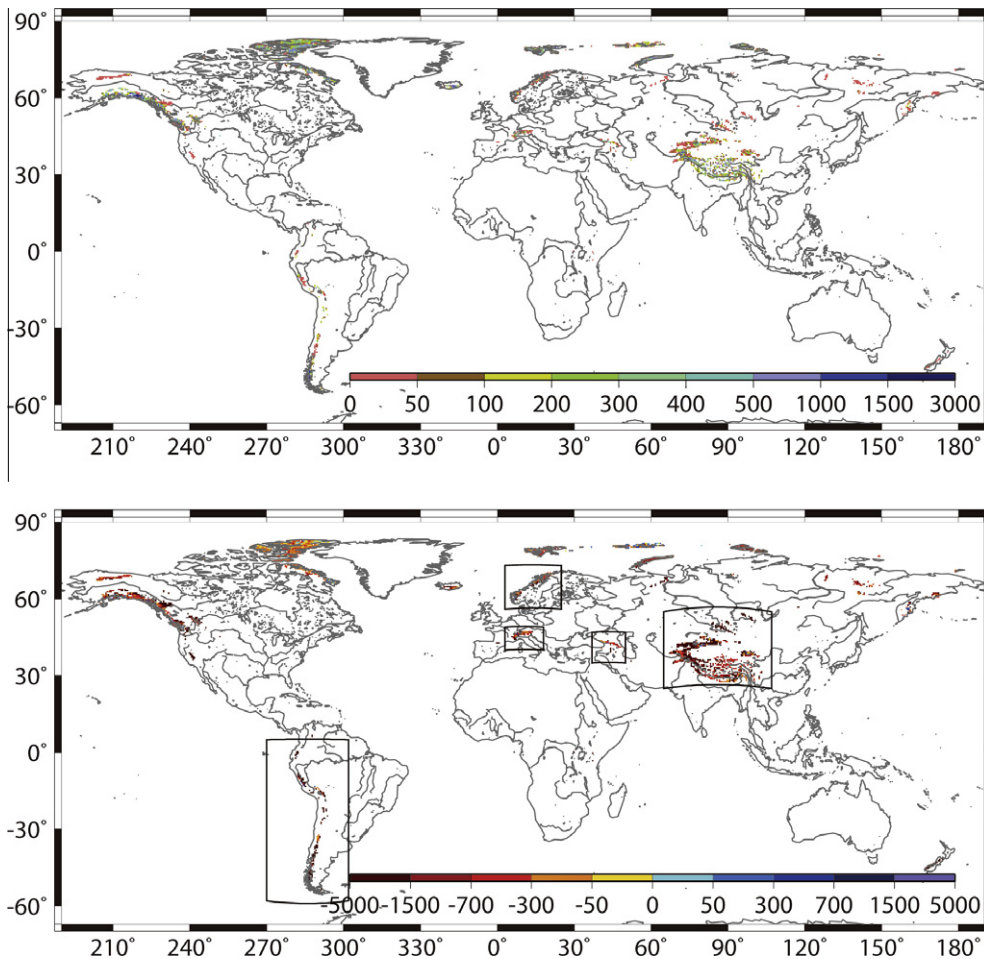


Fig. 6. Global map of modeled glacier area per 0.5° grid cell on the 1st of January 1948, in km^2 (top), and average annual specific mass change of glacier during the 59 yrs from 1948 to 2006, in mm/yr (bottom).

are similar to the values of Lemke et al. (2007), and within the given uncertainty ranges, which do not include uncertainties that derive from uncertainties in the glacier area inventory (Lemke et al., 2007). Both observation-based estimates and HYOGA model

results agree that glacier mass losses have accelerated after 1990, with HYOGA indicating a somewhat stronger acceleration. According to HYOGA, average annual mass losses have increased strongly after the 1990s as compared to the 30 yrs before, with a sea level

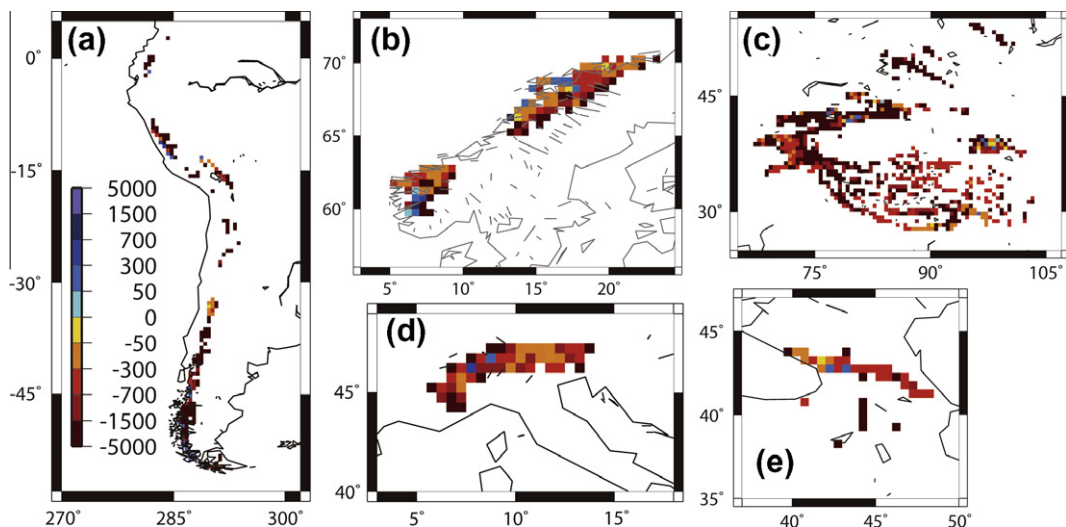


Fig. 7. Enlarged views of average annual specific glacier mass change 1948–2006 (mm/yr) in South America (a), Norway (b), High Mountain Asia (c), Alps (d) and Caucasus (e). Regions are indicated as rectangles in Fig. 6.

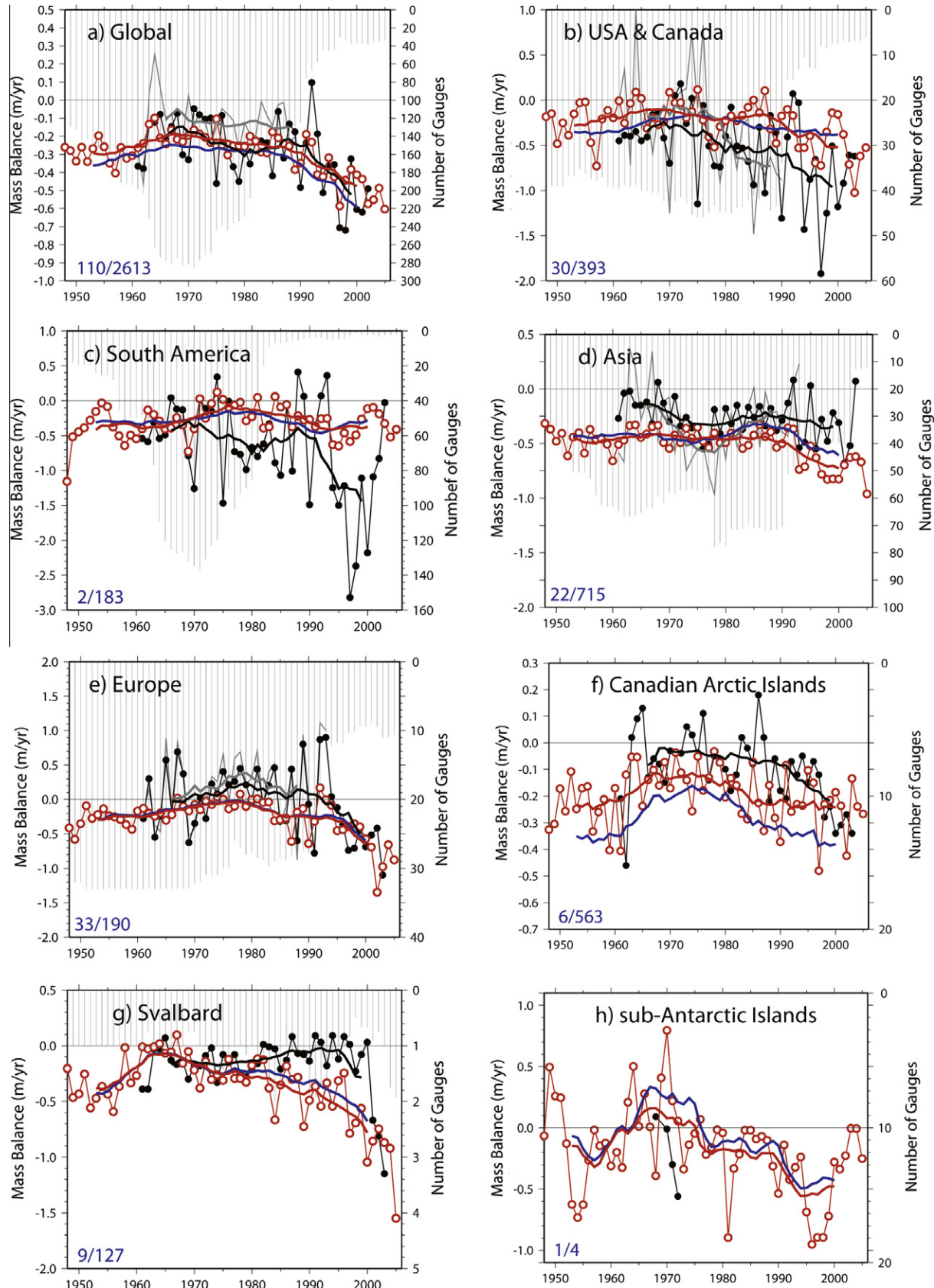


Fig. 8. Time series of regionally averaged annual specific glacier mass balances. Black and grey lines are observations of DM05 and DM97, respectively, and red lines are modeled values. Thick lines are 5-yr moving average. Blue thick lines are 5-yr moving average of mass balance of glacier grid cells where observed mass balances were available within the grid cell. “110/2613” (in blue in the lower left corner of the global analysis box), for example, means that there are 110 observed mass balance values taken into account for constructing the blue lines, and 2613 0.5° grid cells with glaciers in total globally. Grey top-to-bottom bars indicate annual numbers of precipitation gauges used to create daily precipitation input.

Table 2

Global mass balance of glaciers and ice caps outside Greenland and Antarctica. Data of Lemke et al. (2007, their Table 4.4) (LM07) and this study. Assumed glacier area of LM07 is $546 \times 10^3 \text{ km}^2$, while in this study, it is $535 \times 10^3 \text{ km}^2$. Values in parentheses are HYOGA estimations using the LM07 glacier area. Ocean surface area is assumed to be $362 \times 10^6 \text{ km}^2$.

Period	Average annual mass balance				Average annual sea level equivalent (mm/yr)	
	(kg/m ² /yr or mm/yr)		(Gt/yr)		LM07	This study
	LM07	This study	LM07	This study		
1960/61–2003/2004	-283 ± 102	-285	-155 ± 55	$-153 (-156)$	0.43 ± 0.15	$0.42 (0.43)$
1960/61–1989/1990	-219 ± 92	-227	-120 ± 50	$-122 (-124)$	0.33 ± 0.14	$0.34 (0.34)$
1990/91–2003/2004	-420 ± 121	-519	-230 ± 66	$-277 (-282)$	0.63 ± 0.18	$0.76 (0.78)$

rise equivalent of 0.76 mm/yr after 1990, as compared to only 0.34 mm/yr during the 30 yrs before.

4. Discussion

What are possible reasons for the discrepancies between HYOGA results and observed regional averages as shown in Fig. 8 and Table 2? One hypothesis is that the observed regional averages are based on a number of glaciers which is much smaller than the total number of glaciers in a region that was taken into account by HYOGA. Calibration to DM97 regional values did not lead to a close agreement of HYOGA and DM97 regional averages of specific mass losses. For neighboring grid cells, HYOGA may compute very different glacier mass changes.

The blue thick lines in Fig. 8 indicate area-weighted mean mass balances of grid cells in which one of the 110 glaciers with observations used for calibration of HYOGA are located, while 2613 grids are used to obtain mean mass balance in HYOGA (shown in red). Overall, the blue lines are within a few tenths of a meter of the regional averages computed by HYOGA, which indicates that the discrepancies between the regional averages that are based on interpolation of observed mass balances and those that are computed by HYOGA cannot be explained by a bias due to the few observation locations.

Other possible reasons for discrepant regional estimates of glacier mass loss are errors of the HYOGA model results that are caused by the simplistic modeling approach (e.g. modeling all glaciers within a grid cell as one effective glacier) and by inadequate climate input data. Because of the non-linearity in the volume-area relation, inclusion of the glacier area distribution, and possibly different glacier types, within each grid cell rather than treating all glaciers as one appears to be indispensable. HYOGA is expected to underestimate shrinkage of glacierized area and to overestimate glacier volume in regions with many separate small glaciers within a grid cell as it assumes that mass balance of many small glaciers can be simulated by the mass balance of one effective glacier, the area of which is the sum of the areas of the individual glaciers. Including size distribution of glacier area and different glacier types within each grid cell is likely to improve the estimated volume and areal change of glaciers. However, there is currently no inventory that provides such information except for a few grid cells world-wide. Size distribution can be derived directly from satellite imagery and glacier inventories and indirectly from topographic data, using an empirical relationship between size distribution and relief (steepness of landscape) (Raper and Braithwaite, 2005).

In South America, in particular, the number of precipitation gauges that were used to create the gridded precipitation data used as input to HYOGA decreased strongly from about 50–100 before 1980 to less than 10 afterwards (Fig. 8c). With such a small number of observations, we cannot expect to be able to simulate the temporal development of glacier mass loss. The number of precipitation gauges in Canadian Arctic islands, Svalbard and Sub-Antarctic islands are almost zero, indicating that the precipitation

input given for these regions is obtained mainly by extrapolating from surrounding grids or climatologies.

Moreover, the process of glacier calving is not taken into account by HYOGA, such that mass changes of glaciers that do not terminate on land but at the ocean (e.g. in Alaska and South America) are not computed correctly if calving is relevant. Another source of error may be the neglect of firn.

The poor simulation of seasonal mass balances (Fig. 4) and interannual variability (Fig. 5) can partly be explained by the inadequate temperature and precipitation input. Glacier mass changes computed by HYOGA depend strongly on precipitation and near-surface temperature. Climate observations at mountain glaciers are very scarce. Currently, global temperature and precipitation data sets are not suited well for modeling glacier mass balances as they do not represent appropriately the climatic conditions at glaciers. Precipitation stations are rather located in the valleys and not on the mountains, and surface-air temperature at a glacier is expected to be lower than at an ice-free location at the same altitude (Braithwaite and Raper, 2007). This results in an underestimation of the seasonal glacier dynamics by HYOGA (see Fig. 4).

A limited sensitivity analysis was performed to determine the sensitivity of computed glacier mass changes to the scale parameter γ in Eq. (5). (e.g. Radić et al., 2008). When γ was varied by $\pm 30\%$, mass balance within a grid cell changed by less than 1%, after calibration for the individual γ values.

The equilibrium line altitude (ELA) of a glacier is defined as the altitude where accumulation is equal to melting. To validate HYOGA, ELA data at 63 glaciers were obtained from the Glacier Mass Balance Bulletin (WGMS, 2007, and earlier issues). ELA observations may be biased, as low-elevation glaciers are more likely to be observed due to accessibility. The effect of this bias is expected to be small, because ELA is mainly influenced by vertical changes of climate variables. Observed ELAs were averaged if several ELAs were available for a grid cell.

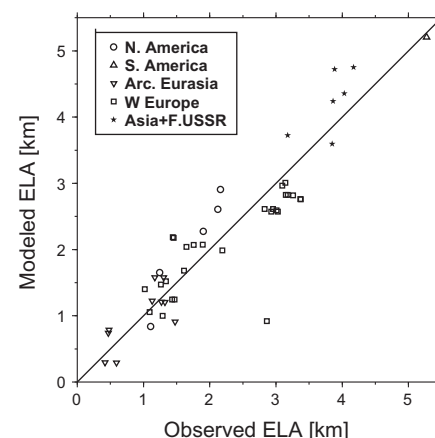


Fig. 9. Correlation between observed and modeled mean equilibrium line altitude (ELA) at 63 locations.

Fig. 9 shows a good agreement of observed and modeled ELA. This indicates that the balance of accumulation and melting at each elevation band is well captured by the model, and that the vertically distributed glacier mass balance is represented well in HYOGA. As the air temperature lapse rate varies according to humidity, Schneeberger et al. (2003) suggested, for a number of glaciers, different temperature lapse rates ranging from -0.1°C to -0.9°C per 100 m. Nevertheless, due to lack of information at the global scale, a uniform lapse rate of -0.65°C per 100 m was applied in HYOGA to estimate temperature at each 50 m elevation band from the mean temperature of the 0.5° grid cell. As is shown in **Fig. 9**, a single lapse rate in HYOGA appears to be sufficient for replicating vertical mass balance change with altitude.

Even though ELA is modeled well, this does not necessarily indicate that the vertical glacier area distribution (Eq. (3)) and the volume-area relation (Eq. (5)) are correctly represented in HYOGA, and these characteristics are decisive for a successful simulation mass changes. In reality, volume-area relationships of glacier vary among glacier types, while a single equation (Eq. (5)) is assumed to describe the relationship in HYOGA.

The vertical sub-grid glacier structure of HYOGA allows for representing several glacier types in different regions of the globe. A glacier mass balance model, for example, that estimates accumulation and melting of glaciers using only the temperature value at a single reference height of glaciers, such as ELA or mean altitude of glacier (e.g. Braithwaite and Raper, 2007), may be difficult to apply to glaciers where both accumulation and melt occur at the same time. HYOGA however, computes mass balances at individual elevation band and thus has the potential to simulate summer accumulation type glaciers (e.g. in High Mountain Asia) that are characterized by accumulation at high elevations and melting at low elevations in the same season.

Using gravimetric data from the GRACE satellites, Matsuo and Heki (2010) estimated glacier mass loss for the Asian high mountain area (Himalaya, Karakorum, Pamir, Tien Shan) of $47 \pm 7 \text{ Gt/yr}$ during 2003–2009. However, they had to rely on a number of highly uncertain assumptions, including a ground water depletion rate in Northern India. Their value compares well to the HYOGA estimate for October 2003–October 2006, with an average mass loss of 37 Gt/yr . For the time period 1961–2003, average glacier mass loss was only 25 Gt/yr according to HYOGA, which is almost equal to the value of from DM05 for the Asian high mountain area (comp. Matsuo and Heki, 2010, their **Fig. 2**).

5. Conclusions

A first global glacier mass balance model was developed that provides gridded sub-annual (daily to monthly) time series of glacier mass changes, glacier ice melting rates and melting rates of snowpack on glaciers for all land areas of the globe except Greenland and Antarctica. With a spatial resolution of 0.5° , HYOGA computes daily snow and glacier mass balance at different elevation bands, which makes it possible to estimate also mass changes of summer accumulation type glaciers where both accumulation and ablation occur in the same seasons. Compared to glacier models that estimate glacier mass changes by using correlations of historical glacier mass balance (integrated over all elevations) with surface temperature and precipitation, HYOGA is better suited for projecting future glacier mass losses. HYOGA has the potential to be coupled to global hydrological or land surface models such that the impact of glacier mass changes on river flow regimes can be taken into account. This will improve the assessment of climate change impacts on freshwater resources.

In accordance with other studies, HYOGA model results show that at the regional scale glaciers have been shrinking at least since

1948. Equally in accordance with other studies, in particular the recent IPCC report (Lemke et al., 2007), global glacier mass losses have accelerated after 1990.

Data on glacier volume are available only for a few glaciers. Due to the simplistic approach for estimating glacier volume, total glacier volumes in HYOGA are not realistic. Therefore, HYOGA cannot be used to estimate the total fresh water stock stored in glaciers or the date when glaciers will disappear due to climate change. Such studies require more detailed and reliable glacier volume estimates which could be derived from information about glacier types, observed glacier thickness, or geomorphological processes.

To improve dynamic glacier mass balance modeling, in particular the simulation of seasonal and interannual mass variations, it will necessary to correct global-scale temperature and precipitation data, by considering local data, such that they better represent the specific conditions at glaciers. Besides, size distribution of glacier area within each grid cell should be included in HYOGA, different glacier types (valley glaciers and ice caps) should be distinguished, and the effect of debris on the glacier surface should be taken into account. Regarding the impact of climate change, inclusion of the impact of radiation on glacier melting may be important, although some of the change due to radiation is indirectly included in the surface temperature change (Ohmura, 2001).

Acknowledgments

We thank Graham Cogley and three anonymous reviewers for their extensive and very helpful comments. This study was partially supported by Grants of Young Scientists A (20686033, 21686045) of the Japan Ministry of Education, Science and Culture and Core Research for Evolutional Science and Technology (CREST), Japan Science and Technology Agency (JST).

References

- Bahr, D.B., Meier, M.F., Peckham, S.D., 1997. The physical basis of glacier volume-area scaling. *Journal of Geophysical Research* 102, 20355–20362.
- Braithwaite, R.J., Raper, S.C.B., 2002. Glaciers and their contribution to sea level change. *Physics and Chemistry of the Earth* 27, 1445–1454.
- Braithwaite, R.J., Raper, S.C.B., 2007. Glaciological conditions in seven contrasting regions estimated with the degree-day model. *Annals of Glaciology* 46, 297–302.
- Chen, J., Ohmura, A., 1990. Estimation of Alpine glacier water resources and their changes since the 1870s. *IAHS Publ.* 193. (*Symposium at Lausanne 1990 – Hydrology in Mountainous Regions I*), pp. 127–135.
- Chen, J.L., Wilson, C.R., Tapley, B.D., Blankenship, D.D., Ivins, E.R., 2007. Patagonia icefield melting by Gravity Recovery and Climate Experiment (GRACE). *Geophysical Research Letters* 34, L22501. doi:10.1029/2007GL031871.
- Cogley, J.G., Adams, W.P., 1998. Mass balance of glaciers other than the ice sheets. *Journal of Glaciology* 44, 315–325.
- Cogley, J.G., 2003. GGHYDRO: Global Hydrographic Data, Release 2.3, Trent Tech. Note 2003-1, Trent Univ., Peterborough, Ont., Canada.
- Cogley, J.G., 2008. Measured rates of glacier shrinkage. *Geophysical Research Abstracts*, 10, EGU2008-A-11595, 2008.
- Cogley, J.G., 2009. A more complete version of the World Glacier Inventory. *Annals of Glaciology* 50, 32–38.
- Döll, P., Kaspar, F., Lehner, B., 2003. A global hydrological model for deriving water availability indicators: model tuning and validation. *Journal of Hydrology* 270, 105–134.
- Dyurgerov, M.B., Meier, M.F., 1997. Mass balance of mountain and subpolar glaciers: a new global assessment for 1961–1990. *Arctic and Alpine Research* 29 (4), 379–391.
- Dyurgerov, M.B., Meier, M.F., 2005. Glaciers and the Changing Earth System: A 2004 Snapshot, Occasional Paper No. 58, Institute of Arctic and Alpine Research, University of Colorado, Colorado, USA, 117pp.
- Fan, Y., van den Dool, H.V.D., 2008. A global monthly land surface air temperature analysis for 1948–present. *Journal of Geophysical Research* 113. doi:10.1029/2007JD008470.
- Fujita, K., Ageta, Y., 2000. Effect of summer accumulation on glacier mass balance on the Tibetan Plateau revealed by mass balance model. *Journal of Glaciology* 46, 244–252.
- Fujita, K., Ohta, T., Ageta, Y., 2007. Characteristics and climatic sensitivities of runoff from a cold-type glacier on the Tibetan Plateau. *Hydrological Processes* 21, 2882–2891.

- Haeblerli, W., Bösch, H., Scherler, K., Østerud, G., Wallén, C.C., 1989. World Glacier Inventory: Status 1988. IAHS (ICSI) – UNEP – UNESCO, Paris.
- Heydernych, C., Salinger, J., Fitzharris, B., Chinn, T., 2004. Annual Glacier Volume in New Zealand 1993–2001. NIWA Report AK02087, National Institute of Water and Atmospheric Research, Auckland, New Zealand, 22 pp.
- Hirabayashi, Y., Kanae, S., Struther, I., Oki, T., 2005. A 100-yr (1901–2000) global retrospective estimation of terrestrial water cycle. *Journal of Geophysical Research* 110, D19. doi:10.1029/2004JD005492.
- Hirabayashi, Y., Kanae, S., Emori, S., Oki, T., Kimoto, M., 2008a. Global projections of changing risks of floods and droughts in a changing climate. *Hydrological Sciences Journal* 53 (4), 754–772.
- Hirabayashi, Y., Kanae, S., Motoya, K., Masuda, K., Döll, P., 2008b. A 59-yr (1948–2006) global meteorological forcing data set for land surface models. Part I: development of daily forcing and assessment of precipitation intensity. *Hydrological Research Letters* 2, 36–40.
- Hirabayashi, Y., Kanae, S., Motoya, K., Masuda, K., Döll, P., 2008c. A 59-yr (1948–2006) global meteorological forcing data set for land surface models. Part II: Global snowfall estimation. *Hydrological Research Letters* 2, 65–69.
- Hock, R., de Woul, M., Radić, V., Dyurgerov, M., 2009. Mountain glaciers and ice caps around Antarctica make a large sea-level rise contribution. *Geophysical Research Letters* 36. doi:10.1029/2008GL037020.
- Hock, R., 2003. Temperature index melt modelling in mountain areas. *Journal of Hydrology* 282, 104–115.
- Huss, M., Farinotti, D., Bauder, A., Funk, M., 2008. Modelling runoff from highly glaciated alpine drainage basins in a changing climate. *Hydrological Processes* 22, 3888–3902.
- Jóhannesson, T., Sigurdsson, O., Laumann, T., Kennett, M., 1995. Degree-day glacier mass-balance modelling with applications to glaciers in Iceland, Norway and Greenland. *Journal of Glaciology* 41, 345–358.
- Lehner, B., Döll, P., Alcamo, J., Henrichs, T., Kaspar, F., 2006. Estimating the impact of global change on flood and drought risks in Europe: a continental, integrated analysis. *Climatic Change* 75, 273–299.
- Lemke, P., Ren, J., Alley, R.B., Allison, I., Carrasco, J., Flato, G., Fujii, Y., Kaser, G., Mote, P., Thomas, R.H., Zhang, T., 2007. Observations: changes in snow, ice and frozen ground. In: Solomon, S., Qin, D., Manning, M., Chen, Z., Marquis, M., Averyt, K.B., Tignor, M., Miller, H.L. (Eds.), *Climate Change 2007: The Physical Science Basis. Contribution of Working Group I to the Fourth Assessment Report of the Intergovernmental Panel on Climate Change*. Cambridge University Press, Cambridge, United Kingdom and New York, NY, USA.
- Matsuo, K., Heki, K., 2010. Time-variable ice loss in Asian high mountains from satellite gravimetry. *Earth and Planetary Science Letters* 290, 30–36.
- Meehl, G.A., Stocker, T.F., Collins, W.D., Friedlingstein, P., Gaye, A.T., Gregory, J.M., Kitoh, A., Knutti, R., Murphy, J.M., Noda, A., Raper, S.C.B., Wetherton, I.G., Weaver, A.J., Zhao, Z.-C., 2007. Global climate projections. In: Solomon, S., Qin, D., Manning, M., Chen, Z., Marquis, M., Averyt, K.B., Tignor, M., Miller, H.L. (Eds.), *Climate Change 2007: The Physical Science Basis. Contribution of Working Group I to the Fourth Assessment Report of the Intergovernmental Panel on Climate Change*. Cambridge University Press, Cambridge, United Kingdom and New York, NY, USA.
- Radić, V., Hock, R., 2010. Regional and global volumes of glaciers derived from statistical upscaling of glacier inventory data. *Journal of Geophysical Research*. doi:10.1029/2009JF001373.
- Radić, V., Hock, R., Oerlemans, J., 2008. Analysis of scaling methods in deriving future volume evolutions of valley glaciers. *Journal of Glaciology* 54, 601–612.
- Raper, S.C.B., Braithwaite, R.J., 2005. The potential for sea level rise: new estimates from glacier and ice cap area and volume distributions. *Geophysical Research Letters* 32, L05502. doi:10.1029/2004GL021981.
- Raper, S.C.B., Braithwaite, R.J., 2006. Low seal level rise projections from mountain glaciers and icecaps under global warming. *Nature* 439. doi:10.1038/nature04448.
- Rees, H.G., Collins, D.N., 2006. Regional differences in response of flow in glacier-fed Himalayan Rivers to climatic warming. *Hydrological Processes* 20, 2157–2169. doi:10.1002/hyp.6209.
- Rignot, E., Rivera, A., Casassa, G., 2003. Contribution of the Patagonia icefields of South America to sea level rise. *Science* 302, 434–437.
- Schneeberger, C., Blatter, H., Abe-Ouchi, A., Wild, M., 2003. Modelling changes in the mass balance of glaciers of the northern hemisphere for a transient $2 \times \text{CO}_2$ scenario. *Journal of Hydrology* 282, 145–163.
- Serreze, M.C., Walsh, J.E., Chapin III, F.S., Osterkamp, T., Dyurgerov, M.B., Romanovsky, V., Oechel, W.C., Morison, J., Zhang, T., Barry, R.G., 2000. Observational evidence of recent change in the northern high-latitude environment. *Climatic Change* 46, 159–207.
- Singh, P., Kumar, N., Arora, M., 2000. Degree-day factors for snow and ice for Dokriani glacier, Garhwal Himalayas. *Journal of Hydrology* 235, 1–11.
- Verbunt, M., Gurtz, J., Jasper, K., Lang, H., Warmerdam, P., Zappa, M., 2003. The hydrological role of snow and glaciers in alpine river basins and their distributed modeling. *Journal of Hydrology* 282, 36–55.
- WGMS, 2007. Glacier Mass Balance Bulletin No. 9 (2004–2005). In: Haeblerli, W., Zemp, M., Hoelzle, M. (Eds.), ICSU (FAGS)/IUGG (IACS)/UNEP/UNESCO/WMO, World Glacier Monitoring Service, Zürich.
- Zhang, Y., Liu, S., Ding, Y., 2006. Observed degree-day factors and their spatial variation on glaciers in western China. *Annals of Glaciology* 43, 301–306.
- Climate Change. Cambridge University Press, Cambridge, United Kingdom and New York, NY, USA.
- Meier, M.F., 1984. Contribution of small glaciers to global sea level. *Science* 226, 1418–1421. doi:10.1126/science.226.4861.1418.
- Mitchell, T.D., Jones, P.D., 2005. An improved method of constructing a database of monthly climate observations and associated high-resolution grids. *International Journal of Climatology* 25, 693–712. doi:10.1002/joc.1181.
- Oerlemans, J., 1993. Modelling of glacier mass balance. In: Peltier, W.R. (Ed.), *Ice in the Climate System*. Springer-Verlag, Berlin and Heidelberg, pp. 101–116.
- Ohmura, A., 2001. Physical basis for the temperature-based melt-index method. *Journal of Applied Meteorology* 40, 753–761.
- Radic, V., Hock, R., 2006. Modeling future glacier mass balance and volume changes using ERA40 reanalysis and climate models: a sensitivity study at Storglaciären, Sweden. *Journal of Geophysical Research* 111, F03003. doi:10.1029/2005JF000440.
- Radić, V., Hock, R., 2010. Regional and global volumes of glaciers derived from statistical upscaling of glacier inventory data. *Journal of Geophysical Research*. doi:10.1029/2009JF001373.
- Radić, V., Hock, R., Oerlemans, J., 2008. Analysis of scaling methods in deriving future volume evolutions of valley glaciers. *Journal of Glaciology* 54, 601–612.
- Raper, S.C.B., Braithwaite, R.J., 2005. The potential for sea level rise: new estimates from glacier and ice cap area and volume distributions. *Geophysical Research Letters* 32, L05502. doi:10.1029/2004GL021981.
- Raper, S.C.B., Braithwaite, R.J., 2006. Low seal level rise projections from mountain glaciers and icecaps under global warming. *Nature* 439. doi:10.1038/nature04448.
- Rees, H.G., Collins, D.N., 2006. Regional differences in response of flow in glacier-fed Himalayan Rivers to climatic warming. *Hydrological Processes* 20, 2157–2169. doi:10.1002/hyp.6209.
- Rignot, E., Rivera, A., Casassa, G., 2003. Contribution of the Patagonia icefields of South America to sea level rise. *Science* 302, 434–437.
- Schneeberger, C., Blatter, H., Abe-Ouchi, A., Wild, M., 2003. Modelling changes in the mass balance of glaciers of the northern hemisphere for a transient $2 \times \text{CO}_2$ scenario. *Journal of Hydrology* 282, 145–163.
- Serreze, M.C., Walsh, J.E., Chapin III, F.S., Osterkamp, T., Dyurgerov, M.B., Romanovsky, V., Oechel, W.C., Morison, J., Zhang, T., Barry, R.G., 2000. Observational evidence of recent change in the northern high-latitude environment. *Climatic Change* 46, 159–207.
- Singh, P., Kumar, N., Arora, M., 2000. Degree-day factors for snow and ice for Dokriani glacier, Garhwal Himalayas. *Journal of Hydrology* 235, 1–11.
- Verbunt, M., Gurtz, J., Jasper, K., Lang, H., Warmerdam, P., Zappa, M., 2003. The hydrological role of snow and glaciers in alpine river basins and their distributed modeling. *Journal of Hydrology* 282, 36–55.
- WGMS, 2007. Glacier Mass Balance Bulletin No. 9 (2004–2005). In: Haeblerli, W., Zemp, M., Hoelzle, M. (Eds.), ICSU (FAGS)/IUGG (IACS)/UNEP/UNESCO/WMO, World Glacier Monitoring Service, Zürich.
- Zhang, Y., Liu, S., Ding, Y., 2006. Observed degree-day factors and their spatial variation on glaciers in western China. *Annals of Glaciology* 43, 301–306.